

ORIGINAL ARTICLE

Comprehensive genetic analyses of relapsed B-cell precursor acute lymphoblastic leukemia in children

Kaori Kubo, Ko Kudo, Tsutomu Toki, Rika Kanazaki,
Fumika Ikeda, Tatsuya Ito, Akie Kobayashi, Tomohiko Sato,
Takuya Kamio, Shinya Sasaki, Kiminori Terui, and Etsuro Ito

Abstract The causes for individual relapse in children with B-cell precursor acute lymphoblastic leukemia (BCP-ALL) remain incompletely understood. Here, we performed comprehensive genetic analyses of 20 pediatric BCP-ALL paired diagnosis-relapse samples. Copy number variation analysis of *IKZF1*, a gene for which deletions are associated with increased relapse risk, revealed deletions at both diagnosis and at relapse (n=5). Targeted next generation sequencing showed that RAS pathway genes including *KRAS* (n=4), *NRAS* (n=2) and *PTPN11* (n=2) were the most common mutations among the sequencing targets at diagnosis and/or relapse. In 7 of 20 cases (35%), mutations in *PTPN11*, *KRAS*, *TP53*, *CTCF*, *NCOR1*, *WHSC1*, *TUSC3*, *ERG* and *NT5C2* were detected only at relapse. Two cases with *TP53* mutations showed fatal outcomes. In two of the four cases with high hyperdiploid BCP-ALL, associated with favorable prognosis, *PTPN11* mutations were detected only at relapse. Targeted RNA sequencing identified a rare subtype of BCP-ALL with a *NUP214-ABL1* fusion that could benefit from tyrosine kinase inhibitors. Together with recent reports that RAS mutations confer sensitivity to MEK inhibitors, these results suggest that comprehensive genetic analysis will contribute to the optimal treatment for relapsed BCP-ALL.

Hirosaki Med. J. 70 : 13–23, 2019

Key words: acute lymphoblastic leukemia; relapse; childhood; RAS pathway genes.

Introduction

Acute lymphoblastic leukemia (ALL) is the most common pediatric cancer^{1,2)}. The advance of risk-stratified chemotherapy for ALL has dramatically improved event-free survival, and aggressive salvage therapies involving allogeneic stem cell transplant have improved overall survival. Despite these improvements, relapse still occurs in around 10-20% of patients and is the leading cause of ALL fatal treatment failure. Recent genomic studies have identified relapse-specific mutations that induce clonal evolution in pediatric ALL³⁻⁵⁾. However, there have been a limited number of studies on relapsed cases with pediatric B-cell precursor ALL (BCP-ALL) in Japan. In this study, we performed a compre-

hensive genetic analysis including a copy number analysis for Ikaros family zinc finger protein 1 (*IKZF1*)⁶⁾ using droplet digital polymerase chain reaction (ddPCR), targeted next generation sequencing covering 25 genes, and targeted RNA sequencing in 20 paired samples at diagnosis, relapse, and remission. Our findings clarify the molecular pathogenesis of childhood relapsed BCP-ALL.

Patients and methods

Patients

Between 1988 and 2016, a total of 20 pediatric patients with BCP-ALL were enrolled in this study. The patients were treated with various protocols including JACLS ALL-02 and JPLSG

ALL B-12 in the Hirosaki University Hospital. The study was conducted in accordance with the Declaration of Helsinki and was approved by the ethics committee at Hirosaki University Graduate School of Medicine.

Copy number variation assay by ddPCR to detect *IKZF1* deletion

Copy Number Variation (CNV) assays for *IKZF1* were conducted using PrimePCR™ ddPCR™ Copy Number Assay primer sets (Bio-Rad, Hercules, USA) and a QX200™ Droplet Digital PCR System (Bio-Rad). The reaction mixtures for ddPCR consisted of the following components: 20-50 ng of gDNA, 11 µL 2 x ddPCR Supermix (Bio-Rad), 1 µL of each *IKZF1* and *EIF2C1* probes, in a final volume of 20 µL. The PCR reaction mixture was prepared in duplicate and loaded into an eight-channel disposable droplet generator cartridge (DG8 cartridge Bio-Rad), with 70 µL of droplet generation oil, into the QX200 Droplet Generator. The generated droplets in a volume of 40 µL were transferred into a 96-well PCR plate and then amplified using optimized following condition: 95°C for 10 minutes, then 43 cycles of 94°C for 30 seconds, 60°C for 60 seconds, and 98°C for 10 minutes. An absolute quantification of each target molecule was analyzed by QuantaSoft Analysis Pro v1.0 software. The chromosomal position of each targeted amplification was previously validated and are as follows: *IKZF1* (hg19 7:50444255-50444377) and *EIF2C1* (hg19 1: 36359351-36359473). The *IKZF1* primer, labeled with FAM dye, targets *IKZF1* exon 4, a region deleted in 98% of acute lymphoblastic leukemia with *IKZF1* deletion⁷⁾. The *EIF2C1* primer, labeled with HEX dye, was used as a reference molecule control. Copy number variation was calculated as the ratio of target molecule to reference molecule concentrations⁸⁾. A total of 29 bone marrow samples in complete remission were analyzed to provide constitutional DNA and sup-

plied a reference mean copy number and standard deviation. We set the threshold of CNV as 1.828-2.104 (1.967+/-4SD, 99.99%, n=29). Data obtained from fewer than 10,000 droplets were excluded.

Gene mutation analysis

Genomic DNA was isolated from paired samples (bone marrow or peripheral blood) at diagnosis, remission, and relapse using the Qiagen Blood mini DNA Kit (Qiagen, Hilden, Germany). We first performed capture-based targeted sequencing covering 23 genes using genomic DNA by the HaloPlex Target Enrichment System (Agilent, Santa Clara, CA, USA) on a MiSeq platform (Illumina, San Diego, CA, USA)³⁾. The custom gene lists are shown in Table 1. CLC Genomic Workbench was used for sequencing alignment to the reference human genome (hg19) and for variant detection. We identified only non-synonymous variants with the following cutoffs: a variant allele frequency (VAF) of >10%, a minimum bi-directional coverage of >10, and an allele frequency of <5% in the normal population (1000 Genomes Project). In addition, we performed mutational analysis of *WHSC1* (*NSD2*)⁹⁾ and *NT5C2*^{4, 5)} by amplicon-sequencing using custom-designed primers and next generation sequencing for the MiSeq. Target amplicons were amplified by KOD plus Neo (TOYOBO, Japan) using optimized parameters: 94°C for 2 minutes, then 30 cycles of 98°C for 10 seconds, 63°C for 30 seconds, and 72°C for 60 seconds. Each library was ligated to an index sequence and subsequently sequenced on the MiSeq platform. The primer sequences are shown in Table 2. To eliminate germline variants, we performed sequencing on bone marrow samples in complete remission as a control.

Targeted RNA sequencing

Total RNA was extracted from bone marrow or blood using the Qiagen Blood RNA Kit (Qia-

Table 1. Gene list for targeted sequencing

| gene | function |
|------------------|-----------------------------|
| <i>KRAS</i> | RAS pathway |
| <i>NRAS</i> | |
| <i>PTPN11</i> | |
| <i>NF1</i> | |
| <i>FLT3</i> | |
| <i>JAK1</i> | Cell signaling |
| <i>JAK2</i> | |
| <i>JAK3</i> | |
| <i>CRLF2</i> | |
| <i>IL7R</i> | |
| <i>PAX5</i> | Transcription factors |
| <i>ERG</i> | |
| <i>SPI1</i> | |
| <i>TCF4</i> | |
| <i>CTCF</i> | |
| <i>TP53</i> | Transcriptional coactivator |
| <i>TUSC3</i> | |
| <i>CREBBP</i> | |
| <i>NCOR1</i> | |
| <i>EZH2</i> | |
| <i>HIST1H2BG</i> | Epigenetics |
| <i>ASMTL</i> | |
| <i>WHSC1</i> | Apoptosis |
| <i>THADA</i> | |
| <i>NT5C2</i> | Drug resistance |

gen, Hilden, Germany). RNA-Seq libraries were prepared using the TruSight™ RNA Pan-Cancer Panel kit (Illumina, San Diego, CA, USA) according to the manufacturer's instructions. The quality of isolated total RNA and cDNA library was analyzed using the Bio-Rad Experion system (Bio-Rad Laboratories, Hercules, CA, USA). An input of 50-100 ng of total RNA was converted to cDNA and then sequenced using the MiSeq platform (Illumina, San Diego, CA, USA). We analyzed the data using the UCSC hg19 reference genome aligners STAR (STAR_2.5.0a) or TopHat (Version 2.0.5), RefSeq annotation, and fusion calling with RNA-Seq alignment software (Illumina, San Diego, CA, USA). Fusion genes were identified as those with a calling score greater than 0.7.

Results

Tested patients

To evaluate genetic alterations in evolutionary process, characteristics of 20 patients with relapsed BCP-ALL were collected and are summarized in Table 3 and Table 4. The male to female ratio was 0.82:1, and the median age at diagnosis was 6.8 years (range, 0.75–16 years), and the median time to relapse was 34 months (range, 4–69 months). Clinical risk, according to the National Cancer Institute (NCI) risk criteria, consisted of 12 cases with high risk and 8 cases with standard risk. Recurrent cytogenetic abnormalities were found in 10 patients (50%): four with high hyperdiploidy, four with t (12;21) (p13;q22), and two with 11q23 rearrangement.

Detection of *IKZF1* deletion by ddPCR

IKZF1 deletions, which are associated with increased relapse risk and poor prognosis⁶⁾, were detected in 5 of 20 samples both at diagnosis and at relapse (Figure 1 and Table 5).

Mutational analysis

Genetic analysis results for our cohort are summarized in Figure 1. Each somatic mutation is listed in Table 6. The mean coverage of deep sequencing of Haloplex analysis was x781, and >95% of target regions were covered over 100-fold (Figure 2A). The mean coverage of tailed PCR-based deep sequencing was x13,980 (Figure 2B). We detected 28 somatic mutations in total, including 5 onset-specific mutations. Mutations in RAS pathway genes and in *TP53* were detected in 7/20 (35%) and 2/20 (10%) cases, respectively. The RAS pathway genes were the most common mutations among the sequencing targets *KRAS* (n=4), *NRAS* (n=2) and *PTPN11* (n=2), and were mutated at diagnosis and/or relapse. These mutations were mutually exclusive. We identified 11 relapse-specific mutations, affecting 7/20 (50%) cases, occurring in genes *PTPN11* (n=2), *TP53*

Table 2. Primer sets and amplicon target regions for tailed PCR

| Gene | Target regions | Amplicon size | Oligo sequence (5'-3') | |
|---------------|---------------------------|---------------|------------------------|-----------------------------|
| WHSC1 Exon 20 | chr4 1962715_1962957 | 243bp | forward | attggcagcacgcttttgcattg |
| | | | reverse | caaagtccagttctacaggtgaccatc |
| WHSC1 Exon 21 | chr4 1976543_1976781 | 239bp | forward | acatgcgattgctaacttgaccga |
| | | | reverse | actctgccccatagccaggagccc |
| NT5C2 Exon 10 | chr10 104856997_104857269 | 340bp | forward | agtgcaaaattctgaatcagctaacc |
| | | | reverse | taggcaaaaataattccactgcataaa |
| NT5C2 Exon 14 | chr10 104852848_104853091 | 311bp | forward | ctcattgttctactctgttggtcaggt |
| | | | reverse | gctggctcatttagatataaattacac |
| NT5C2 Exon 15 | chr10 104851272_104851508 | 304bp | forward | ggtaactgtactcagcatgttagtc |
| | | | reverse | aagtattctgagtaagttttggga |
| NT5C2 Exon 16 | chr10 104850491_104850717 | 294bp | forward | cagttccatccagagcgtattaaggt |
| | | | reverse | gcgaacaggcttccatcatccata |

Table 3. Clinical and biological features

| | |
|---|---------------|
| Total, n | 20 |
| Sex, male, n (%) | 9 (45) |
| Age at relapse, years, n (%) | |
| Median, range | 6.8 (0.75-16) |
| <1 | 1 (5) |
| 1-9 | 11 (55) |
| >10 | 8 (40) |
| Clinical risk group, n (%) | |
| High | 12 (60) |
| Standard/intermediate | 8 (40) |
| Genetic subgroup, n (%) | |
| High hyperdiploidy | 3 (15) |
| 11q23 rearrangement | 2 (10) |
| t(12;21) (p13;q22) | 4 (20) |
| Time to first relapse (month), n (%) | |
| Median, range | 34 (4-69) |
| Extremely early | 5 (25) |
| Early | 3 (15) |
| Late | 12 (60) |
| Site of first relapse, n (%) | |
| Isolated BM | 18 (90) |
| Isolated CNS | 0 |
| Extramedullary | 1 (5) |
| Combined | 1 (5) |
| Stem cell transplantation, n (%) | |
| Yes | 18 (90) |
| No | 2 (10) |
| Outcome of induction therapy, n (%) | |
| Induction failure | 4 (20) |
| Induction death | 0 |
| Second CR | 16 (80) |
| Outcome of patients achieving a second remission, n (%) | |
| Relapsed | 5 (25) |
| Died | 7 (35) |
| Continuing second CR | 11 (55) |

Abbreviation: CR, complete remission, CNS, central nervous system

(n=2), and *KRAS*, *ERG*, *TUSC3*, *CTCF*, *NCOR1*, *WHSC1* and *NT5C2* (one case each). In case 3, we detected two different *NRAS* mutations, G12S at diagnosis, and G12D at relapse (Table 6). However, careful analysis of the onset sample sequence data revealed that the patient had a low burden of *NRAS* G12D mutation (VAF: 0.0818) at diagnosis, and an increase in VAF at onset higher than the detection cutoff.

Fusion genes in relapsed BCP-ALL

We performed targeted RNA sequencing to identify oncogenic fusion genes using the TruSight™ RNA Pan-Cancer Panel kit. The panel targets 1385 cancer-associated genes, including 507 genes involved in fusion and > 850 genes either mutated or deregulated in cancers. At diagnosis, known fusions, including *ETV6-RUNX1* (n=4), *KMT2A-MLL2* (n=2), *ARID1B-ZNF384* (n=1), *NUP214-ABL1* (n=1) and *TCF3-PBX1* (n=1), were detected in 9 of 20 cases (Figure 1). *ARID1B-ZNF384* and *NUP214-ABL1* fusions were validated by Sanger sequencing of reverse transcription PCR products (Figure 3 and Table 7). All of these fusion genes were retained at relapse.

Table 4. Patient characteristics of relapsed BCP-ALL

| Case | Age at diagnosis (y, m) | Gender | WBC at diagnosis (/ μ L) | Time from diagnosis to relapse (m) | Time from therapy-off to relapse (m) | NCI risk | Phase of relapse | Prognosis | Recurrent cytogenetic abnormalities |
|------|-------------------------|--------|------------------------------|------------------------------------|--------------------------------------|----------|------------------|-----------|-------------------------------------|
| 1 | 3y6m | F | 7710 | 31 | 5 | SR | early | dead | t(12;21) (p13;q22) |
| 2 | 0y9m | M | 105770 | 24 | 16 | HR | late | alive | 11q23 rearrangement |
| 3 | 10y3m | F | 1130 | 60 | 33 | HR | late | alive | |
| 4 | 11y6m | F | 305050 | 32 | 17 | HR | late | dead | |
| 5 | 8y0m | F | 2300 | 69 | 39 | SR | late | alive | |
| 6 | 5y7m | F | 1470 | 40 | 10 | SR | late | alive | High hyperdiploid |
| 7 | 4y1m | M | 56860 | 39 | 9 | HR | late | dead | t(12;21) (p13;q22) |
| 9 | 12y1m | F | 4500 | 16 | (-) | HR | extremely early | dead | |
| 10 | 14y8m | F | 40800 | 47 | 23 | HR | late | alive | |
| 12 | 8y4m | M | 1960 | 60 | 34 | SR | late | alive | t(12;21) (p13;q22) |
| 13 | 3y9m | M | | 65 | 40 | SR | late | alive | High hyperdiploid |
| 14 | 12y8m | M | 132860 | 4 | (-) | HR | extremely early | alive | |
| 15 | 1y8m | F | 95100 | 16 | (-) | HR | extremely early | alive | 11q23 rearrangement |
| 18 | 11y2m | M | 35600 | 9 | (-) | HR | extremely early | dead | |
| 20 | 1y0m | M | 17700 | 18 | (-) | HR | extremely early | dead | |
| 21 | 1y10m | F | 12500 | 44 | 15 | SR | late | alive | t(12;21) (p13;q22) |
| 23 | 11y0m | F | 2100 | 32 | 3 | HR | early | dead | |
| 24 | 3y9m | F | 7400 | 28 | 3 | SR | early | alive | High hyperdiploid |
| 25 | 15y7m | M | 12620 | 35 | 9 | HR | late | alive | |
| 26 | 1y10m | M | | 37 | 11 | SR | late | alive | High hyperdiploid |

Abbreviation: y, year; m, month; F, female; M, male; WBC, white blood cell count ; NCI, National Cancer Institute; HR, high risk; SR, standard risk

Discussion

In this study, we performed a comprehensive genetic analysis of 20 paired diagnosis-relapse samples of childhood relapsed BCP-ALL in a single center. Analysis included targeted next generation sequencing covering 25 genes, CNV assays for *IKZF1* deletions by ddPCR, and targeted RNA sequencing. In 7 of 20 (35%) cases, we detected 11 mutations including *TP53*, *PTPN11*, *KRAS*, *ERG*, *TUSC3*, *CTCF*, *NCOR1*, *WHSC1* and *NT5C2* only at relapse. Two cases with multiple relapse specific-mutations including *TP53* resulted in a fatal outcome, consistent with a previous study⁹⁾. The frequency of somatic mutations in relapsed childhood BCP-ALL in a Japanese cohort was similar to previous reports^{3, 9)}.

Gain of function mutations in *NT5C2* induce resistance to 6-mercaptopurine and are selectively present in relapsed ALL^{4, 5)}. The *NT5C2* mutations are present in about 20% of relapsed pediatric T-cell ALL cases⁵⁾ and 3-45% of relapsed BCP-ALL^{4, 5, 9)}. We observed a slightly lower frequency of mutations in *NT5C2* in our cohort of Japanese BCP-ALL patients than the frequencies previously reported from western countries, although the data from both populations are based on low numbers of patients and values showing significant differences between populations are lacking.

In two of the four cases with high hyperdiploid BCP-ALL associated with favorable prognos-

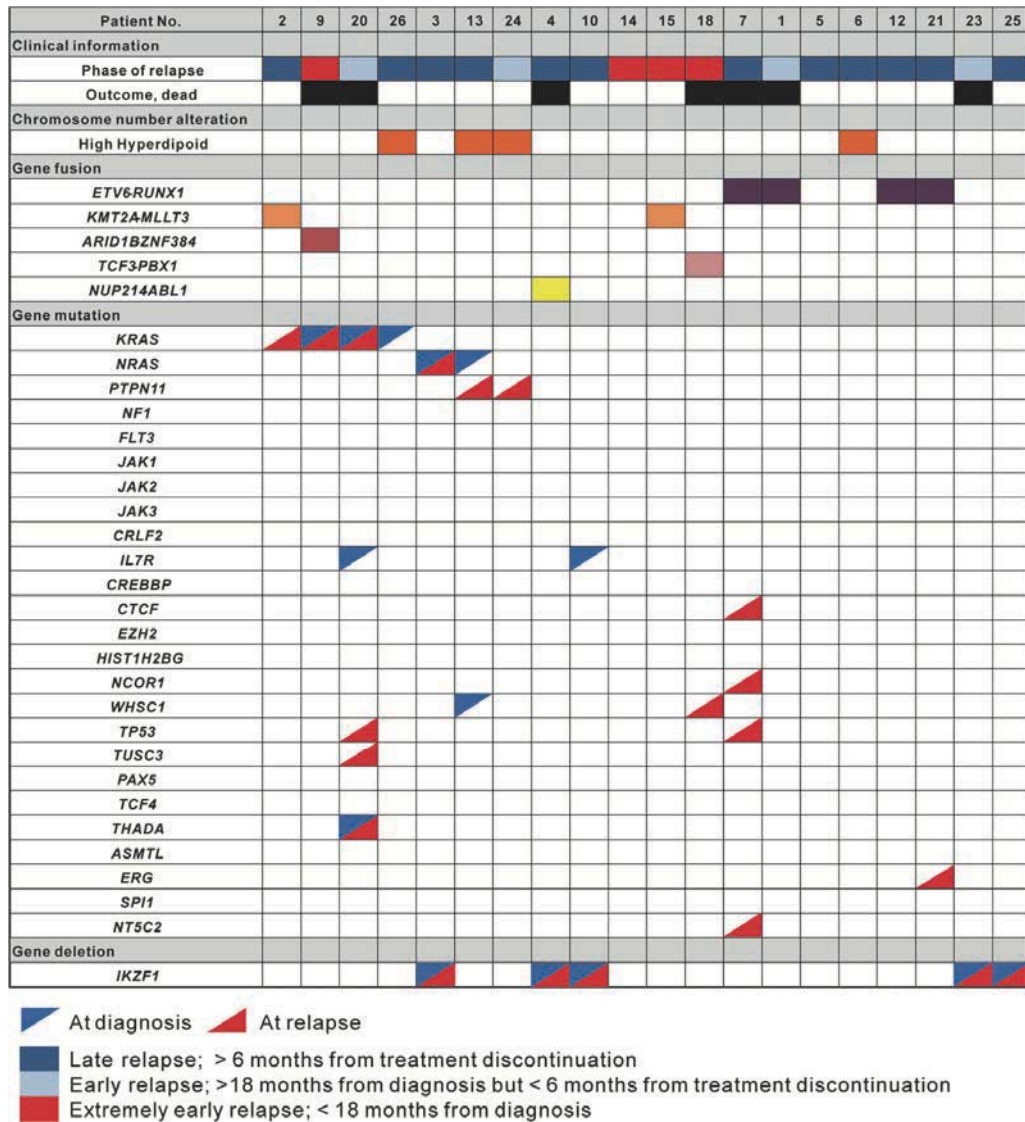


Figure 1 Genetic landscape of childhood BCP-ALL relapse cases.

Clinical information, chromosome number alteration, gene fusions, gene mutations, and deletion of *IKZF1* in 20 paired diagnosis-relapse samples of pediatric BCP-ALL. Somatic mutations at diagnosis and relapse are indicated by blue and red triangles, respectively. Phase of relapse are categorized into late onset, early relapse and extremely early relapse and are indicated by dark blue and right blue and red, respectively.

sis, relapse-specific mutations including *PTPN11* mutations (n=2) were detected. However, in two of four BCP-ALL cases with *ETV6-RUNX1* fusion, another favorable subtype, no additional genetic alterations related to poor prognosis were detected, indicating the potential evolutionary process, which needs to be resolved.

RAS pathway mutations are a common genetic alteration in relapsed ALL and are associated

with high-risk features and poor prognosis. In particular, *KRAS* mutations are associated with reduced overall survival^{10,11}. Indeed, two of four patients with *KRAS* mutations had a fatal outcome in our cohort. *RAS* mutations induce resistance to methotrexate but not to L-asparaginase, daunorubicin, or thiopurines. Furthermore, these mutations show improved response to vincristine^{12,13}. Targeted MEK inhibition with selumetinib showed the clear evidence to reduce leukemic cell

Table 5. Deletion gene copy number measurements of *IKZF1* gene

| case | status onset | CR | relapse | 2nd relapse |
|------|--------------|------|--------------|-------------|
| 1 | 1.96 | 2.03 | 2.02 | 1.99 |
| 2 | 2.09 | 1.99 | 2.01 | |
| 3 | 1.05 | 2.03 | 1.66 | |
| 4 | 1.02 | 2.11 | 0.991 | |
| 5 | 2.05 | 1.95 | 1.99 | 2.02 |
| 6 | 2.03 | 2.02 | 2.09 | 1.98 |
| 7 | 1.96 | 2.08 | 1.96 | 1.95 |
| 9 | 1.96 | 2.00 | 2.06 | |
| 10 | 0.138 | 2.08 | 0.583 | |
| 12 | 2.04 | 2.01 | 2.59 | |
| 13 | 1.98 | 2.03 | 4.77 | |
| 14 | 1.99 | 2.08 | 1.96 | 2.01 |
| 15 | 2.08 | 2.05 | 2.13 | |
| 18 | 2.04 | 2.02 | 2.02 | |
| 20 | 1.88 | 1.99 | 2.06 | |
| 21 | 1.98 | 2.02 | 2.04 | |
| 23 | 1.73 | 2.01 | 1.67 | |
| 24 | 1.97 | 2.06 | 2.01 | |
| 25 | 1.08 | 1.98 | 1.27 | |
| 26 | 1.95 | 1.91 | 1.98 | 1.85 |

Copy number measurements of the gene *IKZF1* by ddPCR on bone marrow samples at diagnosis (onset), in complete remission (CR), and at relapse. CNV values out of normal range are shown in bold.

growth in ALL with RAS pathway mutations, both *in vitro* and *in vivo*¹¹). Furthermore, MEK inhibitors can synergize with prednisolone¹⁴). These findings suggest that patients with RAS pathway mutations could profit from intensification of these drugs and/or MEK inhibitors.

Targeted RNA sequencing identified rare subtypes of BCP-ALL with *ARID1B-ZNF384* (case 9)¹⁵) and *NUP214-ABL1* (case 4) fusions¹⁶). The *NUP214-ABL1* fusion is a recurrent abnormality found in about 6% of T-ALL¹⁶). However, only a few cases with BCP-ALL cases with *NUP214-ABL1* fusion have been reported¹⁷). This subtype belongs to Philadelphia chromosome-like ALL (Ph-like ALL) and is associated with poor outcome. Deletions or mutations of *IKZF1* are a hallmark of both BCR-ABL-positive ALL

and Ph-like ALL. Indeed, our patient (case 4) also harbored *IKZF1* deletion. Notably, Ph-like ALL could benefit from tyrosine kinase inhibitors^{17,18}).

This study has the following limitations: limited total number of patients from a single center, limited target regions for genetic analysis, various treatments in both the first and second lines, and no data regarding minimal residual disease indicating treatment response.

In conclusion, this study identified a number of genetic alterations that are likely to be involved in the pathogenesis of treatment failure in BCP-ALL. These results suggest that comprehensive genetic analyses will contribute to the optimal treatment for relapsed BCP-ALL.

Table 6. List of somatic mutations detected by target sequencing

| Case | Status | Gene | Amino acid change | Allele frequency |
|------|-------------------------------|--------|---------------------|------------------|
| 2 | 1st relapse | KRAS | Q61R | 0.146 |
| 3 | onset | NRAS | G12S | 0.271 |
| 3 | onset | NRAS | G12D | 0.0818 |
| 3 | 1st relapse | NRAS | G12D | 0.143 |
| 3 | 2nd relapse (ethmoid sinuses) | NRAS | G12D | 0.458 |
| 7 | 1st relapse | CTCF | Q131 * | 0.122 |
| 7 | 1st relapse | TP53 | E154 * | 0.504 |
| 7 | 1st relapse | NCOR1 | S2104 * | 0.513 |
| 7 | 2nd relapse | TP53 | E154 * | 0.216 |
| 7 | 2nd relapse | NCOR1 | S2104 * | 0.195 |
| 7 | 2nd relapse | NT5C2 | D415A | 0.184 |
| 9 | onset | KRAS | G13D | 0.194 |
| 9 | 1st relapse | KRAS | G13D | 0.444 |
| 10 | onset | IL7R | T244delinsADAISACD | 0.309 |
| 13 | onset | WHSC1 | V1166G | 0.156 |
| 13 | onset | NRAS | G12D | 0.212 |
| 13 | 1st relapse (testis) | PTPN11 | E76V | 0.359 |
| 18 | relapse | WHSC1 | T1150A | 0.473 |
| 20 | onset | THADA | V30M | 0.455 |
| 20 | onset | IL7R | L248-V258delinsPPYW | 0.125 |
| 20 | onset | KRAS | G12D | 0.419 |
| 20 | 2nd relapse | THADA | V30M | 0.529 |
| 20 | 2nd relapse | TUSC3 | A13V | 0.462 |
| 20 | 2nd relapse | KRAS | G12D | 0.528 |
| 20 | 2nd relapse | TP53 | R116Q | 0.917 |
| 21 | 1st relapse | ERG | V127G | 0.275 |
| 24 | 1st relapse | PTPN11 | T507K | 0.279 |
| 26 | onset | KRAS | G13D | 0.237 |

Conflict of interest

The authors declare that they have no conflict of interest.

Acknowledgment

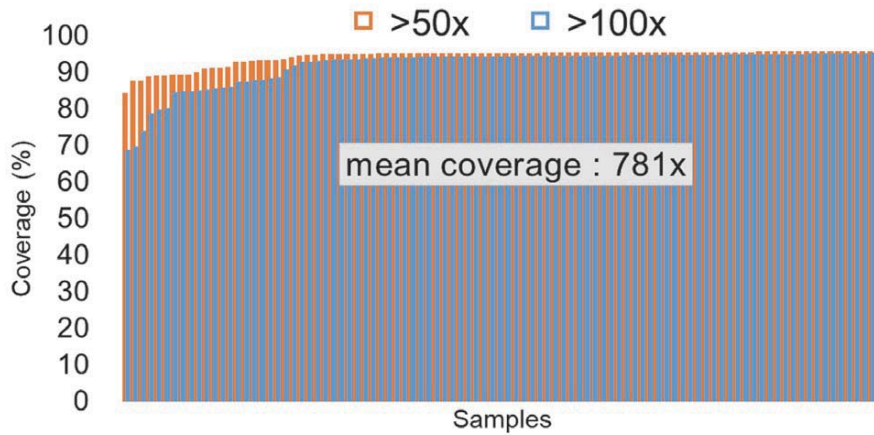
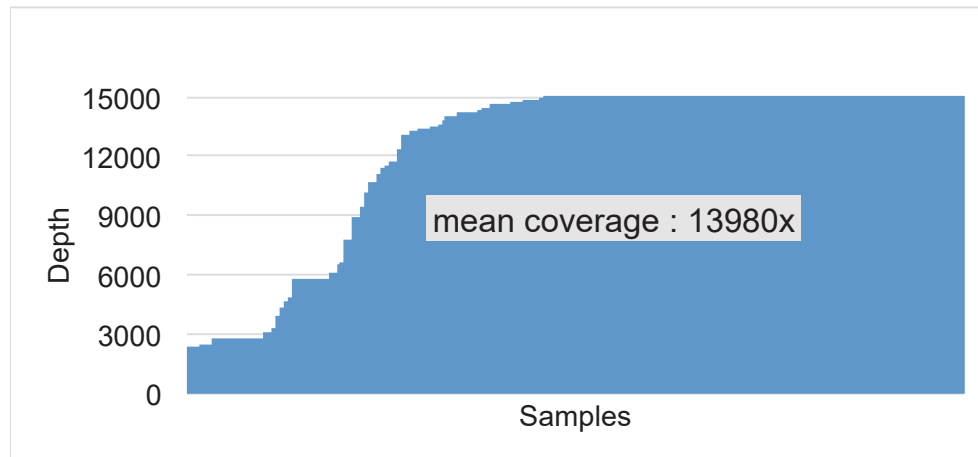
The authors would like to thank H. Kudo, Y. Kudo and A. Mikami for their technical assistance. All authors have no conflicts of interest directly relevant to the content of this article.

Contribution: E.I., T.T. conceived of and designed

the study; K.Kubo, K.Kudo, F.I., T.I., R.K., A.K. and T.T. performed experiments and undertook data analysis and interpretation; K.Kubo, R.K., T.T. performed NGS data analyses; K.Kubo, K. Kudo, T.I., F.I., A.K., T.S., T.K., S.S. and K.T. took care of patients and collected clinical data; K.Kubo, K.Kudo and E.I. wrote the manuscript; and all authors critically reviewed and approved the final manuscript.

References

- 1) Pui CH, Robison LL, Look AT. Acute lymphoblastic leukaemia. *Lancet*. 2008;371:1030-43.

A. Haloplex**B. PCR based deep sequencing****Figure 2** Mean coverage of targeted deep sequencing.

(A) The mean coverage of deep sequencing of Haloplex analysis in total 96 samples. The coverage of coding regions is plotted for each sample. (B) The mean coverage of tailed PCR-based deep sequencing in the total 370 amplicons is shown.

Table 7. Primer sets for RT-PCR analysis of fusion genes

| Gene | Oligo | Sequence (5'-3') |
|---------------|----------------|-------------------------|
| ARID1B-ZNF384 | forward primer | AGCCTTATATGTCGTCCTCAGC |
| | reverse primer | TAGGGTCGATGCTACCTTCTTG |
| NUP214-ABL1 | forward primer | GTTTGGCAGCCCTCCTACTTTT |
| | reverse primer | ACTGTTGACTGGCGTGATGTAGT |

2) Pui CH, Mullighan CG, Evans WE, Relling MV. Pediatric acute lymphoblastic leukemia: where are we going and how do we get there? *Blood*. 2012;120:1165-74.

3) Mullighan, C. G. Zhang J, Kasper LH, Lerach S,

Payne-Turner D, Phillips LA, Healtley SL, et al. CREBBP mutations in relapsed acute lymphoblastic leukaemia. *Nature*. 2011;471:235-9.

4) Meyer JA, Wang J, Hogan LE, Yang JJ, Dandekar S, Patel JP, Tang Z, et al. Relapse-specific muta-

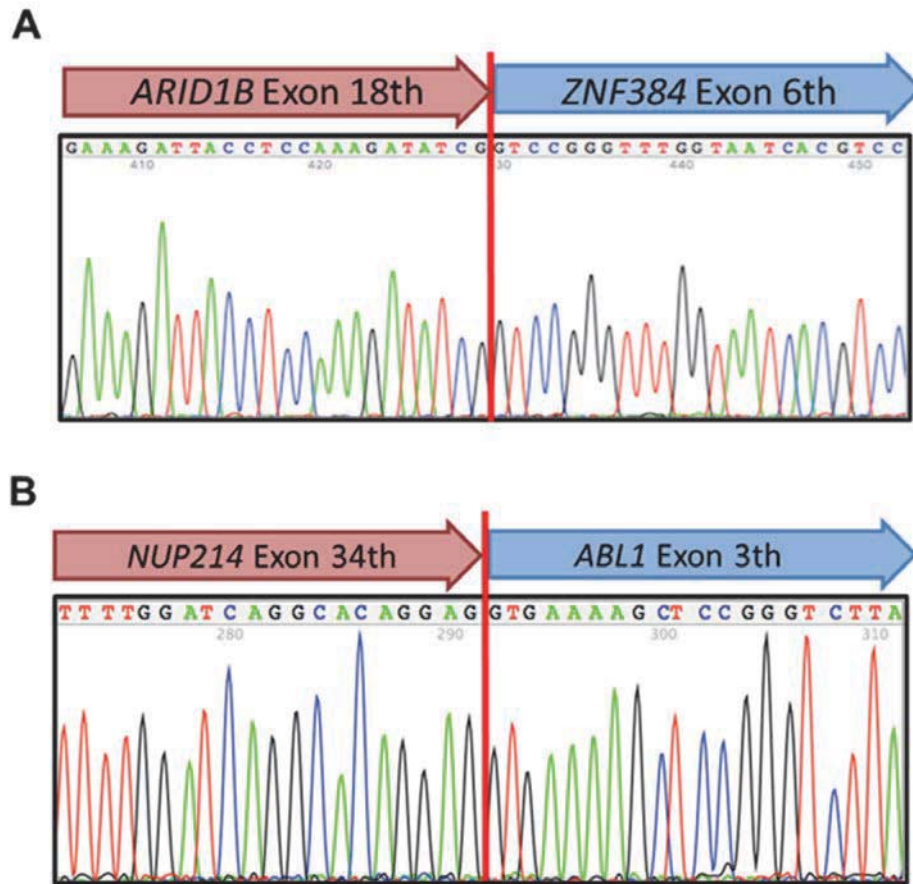


Figure 3 Rare subtypes of BCP-ALL with *ARID1B-ZNF384* and *NUP214-ABL1* fusion. Sequencing analysis of RT-PCR products of *ARID1B-ZNF384* (A) and *NUP214-ABL1* fusions (B)

- tions in *NT5C2* in childhood acute lymphoblastic leukemia. *Nat Genet.* 2013;45:290-4.
- 5) Tzoneva G, Perez-Garcia A, Carpenter Z, Khiabani H, Tosello V, Allegretta M, Paietta E, et al. Activating mutations in the *NT5C2* nucleotidase gene drive chemotherapy resistance in relapsed ALL. *Nat Med.* 2013;19:368-71.
 - 6) Mullighan CG, Su X, Zhang J, Radtke I, Phillips LA, Miller CB, Ma J, et al. Deletion of *IKZF1* and Prognosis in Acute Lymphoblastic Leukemia. *N Engl J Med.* 2009;360:470-80.
 - 7) de Smith AJ, Walsh KM, Hansen HM, Endicott AA, Wiencke JK, Metayer C, Wiemels JL. Somatic Mutation Allelic Ratio Test Using ddPCR (SMART-ddPCR): An Accurate Method for Assessment of Preferential Allelic Imbalance in Tumor DNA. Toland AE, ed. *PLoS One.* 2015;10: e0143343.
 - 8) Iacobucci I, Storlazzi CT, Cilloni D, Lonetti A, Ottaviani E, Soverini S, Astolfi A, et al. Identification and molecular characterization of recurrent genomic deletions on 7p12 in the *IKZF1* gene in a large cohort of BCR-*ABL1*-positive acute lymphoblastic leukemia patients: on behalf of Gruppo Italiano Mal. Blood. 2009;114:2159-67.
 - 9) Ma X, Edmonson M, Yergeau D, Muzny DM, Hampton OA, Rusch M, Song M, et al. Rise and fall of subclones from diagnosis to relapse in pediatric B-acute lymphoblastic leukaemia. *Nat Commun.* 2015;6:6604.
 - 10) Malinowska-Ozdowy K, Frech C, Schönegger A, Eckert C, Cazzaniga G, Stanulla M, zur Stadt U, et al. *KRAS* and *CREBBP* mutations: a relapse-linked malicious liaison in childhood high hyperdiploid acute lymphoblastic leukemia. *Leukemia.* 2015;29:1656-67.

- 11) Irving JA, Enshaei A, Parker CA, Sutton R, Kuiper RP, Erhorn A, Minto L, et al. Integration of genetic and clinical risk factors improves prognostication in relapsed childhood B-cell precursor acute lymphoblastic leukemia. *Blood*. 2016;128:911-22.
- 12) Oshima K, Khiabani H, da Silva-Almeida AC, Tzoneva G, Abate F, Ambesi-Impiombato A, Sanchez-Martin M, et al. Mutational landscape, clonal evolution patterns, and role of RAS mutations in relapsed acute lymphoblastic leukemia. *Proc Natl Acad Sci U S A*. 2016;113:11306-11.
- 13) Jerchel IS, Hoogkamer AQ, Ariès IM, Steeghs EMP, Boer JM, Besselink NJM, Boeree A, et al. RAS pathway mutations as a predictive biomarker for treatment adaptation in pediatric B-cell precursor acute lymphoblastic leukemia. *Leukemia*. 2018;32:931-40.
- 14) Ariès IM, van den Dungen RE, Koudijs MJ, Cuppen E, Voest E, Molenaar JJ, Caron HN, et al. Towards personalized therapy in pediatric acute lymphoblastic leukemia: RAS mutations and prednisolone resistance. *Haematologica* 2015;100:e132-e136.
- 15) Shago M, Abal O, Hitzler J, Weitzman S, Abdelhaleem M. Frequency and outcome of pediatric acute lymphoblastic leukemia with *ZNF384* gene rearrangements including a novel translocation resulting in an *ARID1B/ZNF384* gene fusion. *Pediatr Blood Cancer*. 2016;63:1915-21.
- 16) Graux C, Cools J, Melotte C, Quentmeier H, Ferrando A, Levine R, Vermeesch JR, et al. Fusion of *NUP214* to *ABL1* on amplified episomes in T-cell acute lymphoblastic leukemia. *Nat Genet*. 2004;36:1084-9.
- 17) Duployez N, Grzych G, Ducourneau B, Fuentes MA, Gardel N, Boyer T, abou Chahla W, et al. *NUP214-ABL1* fusion defines a rare subtype of B-cell precursor acute lymphoblastic leukemia that could benefit from tyrosine kinase inhibitors. *Haematologica*. 2016;101:e133-134.
- 18) Roberts KG, Li Y, Payne-Turner D, Harvey RC, Yang YL, Pei D, McCastlain K, et al. Targetable Kinase-Activating Lesions in Ph-like Acute Lymphoblastic Leukemia. *N Engl J Med*. 2014;371: 1005-15.